Uniosun Journal of Engineering and Environmental Sciences (UJEES), Vol. 8 No. 2, Sept., 2026
DOI: 10.64980/ujees.v8i2.017 **Afolalu et al.**
Published: September 30, 2026

ENABLING THE 6G DIGITAL REVOLUTION THROUGH CELL-FREE NETWORKS: PERFORMANCE GAINS OVER CONVENTIONAL CELLULAR ARCHITECTURES

Oladele Felix AFOLALU[1*], Tolulope Tola AWOFOLAJU[2], Moses Olumuyiwa OLLA[3], Funmilola Margaret ADEAGBO[4], Abdulsemiu Alabi OLAWUYI[5], Olalekan Mudasiru BADA[6], Muyideen Olalekan LAWAL[7], Kehinde Olukunmi ALAWODE[8], Hammed Oyebamiji LASISI[9] and Titus Oluwasuji AJEWOLE[10]

[1,2,3,4,5,6,7,8,9,10]*Department of Electrical and Electronic Engineering, Osun State University, Osogbo*

[*]Corresponding Author*: oladele.afolalu@uniosun.edu.ng*

Abstract
The evolution toward sixth-generation (6G) wireless communication requires network architectures capable of supporting high data rates, low latency, reliable coverage and massive connectivity. However, the service quality of currently operated cellular networks is unreliable due to the significant variations within each cell. Hence, a cell-free network architecture which guarantees increased peak rates to the great majority of the areas throughout the geographical coverage area for future mobile networks is proposed. In this paper, a cell-free network is exploited to achieve higher and more uniform signal-to-interference-plus noise ratio (SINR) within the coverage area. Additionally, the cell-free network is combined with massive multiple-input multiple-output (mMIMO) technology envisioned for beyond fifth generation (B5G) cellular networks to further mitigate interference through joint processing at multiple access points (APs). Under a noise power of −86.98 dBm, simulation results show that cell-free mMIMO performs better than small cells networks by producing a gap of 4dB in the upper 95% probable SINR of the CDF curve. In addition, relative to the conventional cellular architecture, the proposed cell-free mMIMO system achieves a 32.24% improvement in average spectral efficiency, a 32.12% increase in average user throughput and a 233.22% improvement in 5th-percentile throughput, demonstrating substantial gains in both average and cell-edge user performance. The architecture also reduces average latency by 82.70%, while increasing coverage probability by 135.71%, from 17.50% to 41.25%. However, due to the implementation complexity of cell-free mMIMO, it is recommended that a robust user-centric AP selection and clustering algorithm be designed to reduce the backhaul.

Keywords
Access point, beyond 5G, cellular network, massive MIMO, signal-to-noise-ratio, 6G

1. INTRODUCTION

Over the decades, the wireless communication services have utilised the cellular network topology as conventional way of covering a large geographical area. In the setup, a set of user equipment (UEs) is served by each base station [1], [2], [3], [4]. Consequently, this has led to improved spectral efficiency (SE) through reduction in sizes of the cells and using signal processing with advanced techniques for interference reduction.

In recent years, massive multiple-input multiple-output (mMIMO) has received great attention as a significant physical layer scheme for beyond-fifth generation (B5G) technology. It is expected that the SE will be improved by at least 10× over conventional cellular networks, replacing the ultra-dense deployment approach with an upgraded base station (BS) hardware [5], [6]. Thus, the SE gain is realised from incorporating the BS with a hundred or more antenna of compact array. The antennas are used to spatially multiplex many UEs and for digital beamforming of same resources in the time-frequency domain. As compared to the traditional multi-user MIMO, mMIMO is characterized by many more antennas at the BS than UEs in the cell. Hence, to reduce intra- and inter-cell interference within the network, minimum mean-squared error (MMSE) combining can be used as advanced signal processing techniques, on each BS in the uplink [7], [8].

Current research works on cell-free network focus on joint implementation with mMIMO technology. In the work of [9], downlink cell-free mMIMO systems were considered where a significant number of distributed access points (APs) were serving a considerably smaller number of users at the same time. Transmission of

data to all users was facilitated through conjugate beamforming while individual AP employs local channel estimates based on uplink pilots received. Thereafter, the authors desired a remarkable quality of service (QoS) to be provided equally to all authentic users by deriving a closed-form expression to estimate the achievable rate. This is in addition to designing a max-min power control scheme that is optimally guaranteed. By comparison, performance evaluation between conventional small-cell and cell-free networks showed a considerable improvement in the throughput, while providing a stronger shadow correlation fading compared to small-cell networks.

To also analyse how cell-free performance is affected by backhaul network, [10], [11], [12] implemented a limited-backhaul cell-free mMIMO for the purpose of information sharing between the central processing unit (CPU) and the APs in fog radio access network (F-RAN)-enabled setup [10]. The work is a follow up of the methodology used in [13]. To show that limited-backhaul cell-free mMIMO performs better than cell-free mMIMO with perfect backhaul links, the authors utilized a few bit for channel estimation and quantization of the received signals by exploiting microwave wireless backhaul links. Furthermore, the ergodic achievable rates were derived to provide a robust analysis. In reality, implementing cell-free mMIMO having limited backhaul links can actually be challenging, especially in the uplink. This is due to the extra self-interference introduced to the CPU signals, as a result of the CPU receiving quantized version of the signal at the APs, by the limited backhaul links. Hence, the total amount required for data rate transmission of the aforementioned quantized signals that will sufficiently be accurate, such that performance degradation is avoided is much more than the allowable total user data rate of those signals. The number is estimated to be 20–50 times the equivalent data rate over optical fiber, utilizing the common public radio interface (CPRI) standard [14].

Similarly, [11] proposed an AP clustering optimization method by considering CPU resources such as distance, channel condition, power, bandwidth and data demands of APs. The aim is to maximize network performance and resolve scalability challenge by balancing channel conditions. However, signal distortion due to backhaul link capacity can significantly impact system performance. The authors in [12] addressed this challenge by proposing a joint distortion aware clustering (DAC) and distortion-aware adaptive clustering (DAAC) methods. Performance evaluation of both methods against baseline proximity-based clustering (PC) approach showed DAC and DAAC to outperform PC in terms of fairness, SE and robustness against distortion.

The most recent work on cell-free system is an advancement of open radio access network (ORAN) on 5G and beyond mobile communications [15], [16], [17]. The authors in [15] demonstrated cell-free mMIMO as a promising evolutionary technology of the sixth generation (6G) networks. The work focused on the development of a prototype open-source software components to serve 5G UEs. With cell-free mMIMO, the peak rate, reliability and spectrum efficiency of wireless communication system can be effectively improved. By combining cell-free mMIMO with ORAN architecture, implementation issues such as time-frequency synchronization, ORAN radio units (O-RU), low layer splitting and artificial intelligent (AI)-based user associations, among others are investigated through theoretical analysis and numerical simulation [18]. Essentially, the work in [16] outlined the need for user-centric cell-free mMIMO as a candidate technology for 6G networks. Some of the benefits highlighted include enhanced energy efficiency, improved service quality and increased coverage probability. These enhancements are sustainable for ORAN's architectural programmability and disaggregation in 6G applications. Generally, the deployment of cell-free mMIMO is mainly mitigated by cost and capacity-limited fronthaul links. As a result, [17] proposed a two-tiered optimization framework for cost-effective hybrid fronthaul planning. The approach is an integration of several intelligent algorithms to accommodate network configurations and decentralized processing levels.

In this paper, the benefit of cell-free networks over conventional cellular system is presented for enhanced signal-to-interference-plus noise ratio (SINR), SE, latency and coverage probability.

The specific contributions of this paper are summarized as follows.

1. Development of a comparative framework to evaluate cell-free mMIMO against traditional cellular architecture, taking into consideration the deployment, propagation, bandwidth, transmit power and user distribution conditions. The aim is to establish a fair basis for quantifying the implementation gains, achievable through distributed AP cooperation.
2. Formulation of a unified mathematical model to characterize both the cell-free mMIMO and conventional cellular networks in terms of the received signal, channel model, beamforming, SINR and SE.
3. Evaluation of average and user-level SE to establish how distributed AP cooperation in cell-free mMIMO can improve spectral utilization, compared with conventional cellular scenario.
4. Establishment of a multi-dimensional performance evaluation framework for 6G network under key performance indicators (KPIs), such as SE, latency, throughput and coverage probability, unlike studies that focus on a single KPI. This aligns with the vision of cell-free MIMO as a candidate scheme for B5G and 6G networks.

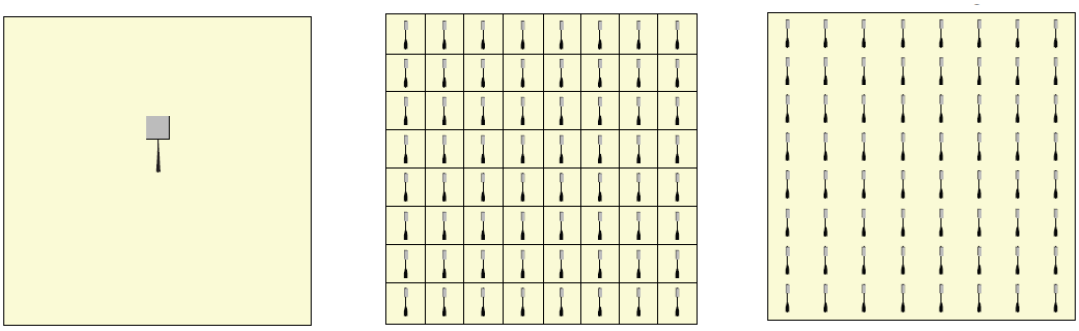
2. MATERIALS AND METHOD

2.1 System Model

Consider a system comprising a single-cell mMIMO configuration where the AP has M = 64 antennas, such that $m = [1, \dots, M]$ as shown in Figure 1(a). This is a typical representation of a cellular network comprising single cell. Let $g = [g_1 \dots g_M]^T \in \mathbb{C}^M$ represent the channel response between the M antennas and K UE, where $k = [1, \dots, K]$. Thus, signal $\boldsymbol{y}^{\text{MIMO}} \in \mathbb{C}^M$ received by the AP in the uplink will be

$$\mathbf{y}^{\text{MIMO}} = \mathbf{g}s + \mathbf{n} \tag{1}$$

such that $s \in \mathbb{C}$ denotes the information signal having transmit power $\mathbb{E}\{|s|^2\} = p$, while $\mathbf{n} \sim \mathcal{N}_{\mathbb{C}}(\mathbf{0}_M, \sigma_{\text{ul}}^2 \mathbf{I}_M)$ represents noise at the receiver, and σ_{ul}^2 is the noise power.



(a) (b) (c)

Figure 1: Three basic setups. (a) One cell with a single AP equipped with M = 64 antennas (b) Cellular setup with 64 APs each having a single antenna, while a UE will only be served by one AP and (c) Cell-free mMIMO setup with the same L = 64 APs as in (b), but the APs are cooperating to serve the UE.

It is noteworthy that the AP will have to estimate s, which can only be achieved through the application of a receive combining vector $\mathbf{v} \in \mathbb{C}^M$ to (1), hence we have

$$\hat{s}^{\text{MIMO}} = \mathbf{v}^{\text{H}} \boldsymbol{y}^{\text{MIMO}} = \mathbf{v}^{\text{H}} \mathbf{g}s + \mathbf{v}^{\text{H}} \mathbf{n} \tag{2}$$

From (2), the signal-to-noise ratio (SNR) can be expressed as [19]

$$\frac{\mathbb{E}\left\{\left|\mathbf{v}^{\text{H}} \mathbf{g}s\right|^2\right\}}{\mathbb{E}\left\{\left|\mathbf{v}^{\text{H}} \mathbf{n}\right|^2\right\}} = \frac{p}{\sigma_{\text{ul}}^2} \frac{\left|\mathbf{v}^{\text{H}} \mathbf{g}\right|^2}{\|\mathbf{v}\|^2} \tag{3}$$

In order to maximize the SNR, the AP can conveniently choose **v** based on the channel **g**. From Cauchy-Schwartz inequality, it follows that when **v** and **g** are parallel vectors, (3) are maximized. Subsequently, to obtain the maximum SNR, the unit-norm maximum ratio combining (MRC) vector $\mathbf{v} = \mathbf{g}/||\mathbf{g}||$ can be employed such that

$$\text{SNR}^{\text{MIMO}} = \frac{p}{\sigma_{\text{ul}}^2} ||\mathbf{g}||^2 \tag{4}$$

We assume co-location of all the antennas in a big array at the AP, so that all the antennas and UE possess identical propagation distance d. Thus, using the large-scale fading model

$$\beta(d)\ [\text{dB}] = -30.5 - 36.7 \log_{10}\left(\frac{d}{1\text{m}}\right) \tag{5}$$

and setting $|g_m|^2 = \beta(d)$ for $m = 1, \dots, M$, we obtain

$$\text{SNR}^{\text{MIMO}} = \frac{p}{\sigma_{\text{ul}}^2} M\beta(d) \tag{6}$$

Equation (6) is a direct implication of proportionality between the SNR and number of antennas M in a single-cell mMIMO network.

For comparison purpose, the above scenario can be extended to a cellular setup with small cells, comprising geographically distributed $L = 64$ APs, shown in Figure 1(b), such that $l = [1, \dots, L]$. Unlike the previous case where $M = 64$, here, a single antenna is installed in each AP, which will serve the UE only.

Hence, the expected channel response experienced between the UE and lth AP is denoted as $h_l \in \mathbb{C}$, while the signal $y_l^{sc} \in \mathbb{C}$ received at AP l in the uplink is given as

$$y_l^{sc} = h_l s + n_l \tag{7}$$

such that $s \in \mathbb{C}$ corresponds to the information from the signal satisfying the condition $\mathbb{E}\{|s|^2\} = p$ and $n_l \sim \mathcal{N}_{\mathbb{C}}(0, \sigma_{ul}^2)$ denotes the receiver noise. Hence, the SNR at the lth AP is expressed as

$$\text{SNR}_l^{sc} = \frac{\mathbb{E}\{|h_l s|^2\}}{\mathbb{E}\{|n_l|^2\}} = \frac{p}{\sigma_{ul}^2}|h_l|^2 \tag{8}$$

Ideally, the UE will choose only one of the APs considering the traditional nature of cellular network where cooperation among the APs is not guaranteed. In this manner, it is the common practice for the UE to automatically choose the AP capable of providing the strongest SNR. Thus, the UE experiences SNR corresponding to

$$\text{SNR}^{sc} = \max_{l \in \{1,\dots,L\}} \text{SNR}_l^{sc}$$

$$= \frac{p}{\sigma_{ul}^2} \max_{l \in \{1,\dots,L\}} |h_l|^2 \tag{9}$$

If the distance, i.e. the separation, between the lth AP and UE is represented by d_l and $|h_l|^2 = \beta(d_l)$, then the SNR becomes

$$\text{SNR}^{sc} = \frac{p}{\sigma_{ul}^2} \max_{l \in \{1,\dots,L\}} \beta(d_l) \tag{10}$$

Finally, at this point, the benefit obtained from the cell-free mMIMO scheme can easily be demonstrated by imitating the small-cell setup with the same $L = 64$ APs (see Figure 1(c)). However, one of the major differences here is that the APs are allowed to cooperate while serving the UE. Hence, the received signals in (7) can jointly be written as

$$\mathbf{y}^{cf} = \mathbf{h}s + \mathbf{n} \tag{11}$$

where $\mathbf{h} = [h_1 \dots h_L]^T$ and $\mathbf{n} = [n_1 \dots n_L]^T$. Similarly, the receive combining vector $\mathbf{v} \in \mathbb{C}^L$ used for the single-cell mMIMO scenario discussed above can be applied to (11) for the estimation of s, which results to

$$\hat{s}^{cf} = \mathbf{v}^H \mathbf{y}^{cf}$$

$$= \mathbf{v}^H \mathbf{h} s + \mathbf{v}^H \mathbf{n} \tag{12}$$

Comparing (12) with similar structure in (2), it can be deduced that MRC with $\mathbf{v} = \mathbf{h}/||\mathbf{h}||$ will produce maximum SNR as

$$\text{SNR}^{cf} = \frac{p}{\sigma_{ul}^2}||\mathbf{h}||^2$$

$$= \frac{p}{\sigma_{ul}^2} \sum_{l=1}^{L} |h_l|^2 \tag{13}$$

When (13) is compared with the expression derived for small-cell network in (9), it will be noticed that there is a proportional relationship between the SNR obtained by the cell-free network and the expression $\sum_{l=1}^{L}|h_l|^2$. On the contrary, the most significant term in the sum is shared by the small-cell arrangement. However, if the cell-free network is compared with the single-cell mMIMO network, we can spot the difference in the channels **h** and **g**. It can be seen that the SNRs for both are respectively proportional to $\|\mathbf{h}\|^2$ and $\|\mathbf{g}\|^2$. In other to conclude which of these two squared values is larger, we rely on comparison through simulations. Since d_l represents the distance, as stated earlier, from the UE to lth AP, the expression for the SNR will be written from (13) as

$$\text{SNR}^{cf} = \frac{p}{\sigma_{ul}^2} \sum_{l=1}^{L} \beta(d_l) \tag{14}$$

2.2 Achievable Rate

In other to analyse the achievable rate of both the small cell and cell-free networks, our first assumption is to imagine the CPU as utilizing only the channel statistical information during detection. Hence, the achievable rate obtained through a rigorous closed-form expression can be obtained as follows:
For the small cell, the achievable rate is given as

$$\mathrm{R^{sc}} = \log_2(1 + \mathrm{SNR^{sc}})$$

$$= \log_2\left(1 + \frac{p}{\sigma_{\mathrm{ul}}^2} \max_{l\in\{1,\ldots,L\}} \beta(d_l)\right) \tag{15}$$

Similarly, the achievable rate for the cell-free network can be expressed as

$$\mathrm{R^{cf}} = \log_2(1 + \mathrm{SNR^{cf}})$$

$$= \log_2\left(1 + \frac{p}{\sigma_{ul}^2} M\beta(d_l)\right) \tag{16}$$

Taking into consideration interference between concurrent transmissions in the presence of multiple UEs, the above analysis is extended to evaluate the impact of coverage probability, SE and latency on the network. This is important as it shows the key benefit and the ability of cell-free network to manage interference by joint processing at multiples APs. However, this advantage is nonexistent in cellular networks having an equally dense deployment of APs.

As stated earlier, in the traditional cellular network, each user is associated with its nearest BS, while all APs jointly serve all UEs through coherent transmission in the cell-free architecture.

Hence, the received signal for user *K* in the cell-free network can be expressed as

$$y_k = \sum_{l=1}^{L} \sqrt{p_l}\, \mathbf{h}_{lk}^H \mathbf{w}_{lk} s_k + n_k \tag{17}$$

where $\mathbf{w}_{lk}$ is the beamforming vector, while the corresponding SINR is computed as

$$\mathrm{SINR}_k = \frac{\left|\sum_l \sqrt{p_l}\mathbf{h}_{lk}^H \mathbf{w}_{lk}\right|^2}{\sum_{i\neq k}\left|\sum_l \sqrt{p_l}\mathbf{h}_{li}^H \mathbf{w}_{li}\right|^2 + \sigma^2} \tag{18}$$

Thus, the achievable SE η is

$$\eta_k = \log_2(1 + \mathrm{SINR}_k) \tag{19}$$

$$\overline{\eta} = \frac{1}{K}\sum_{k=1}^{K} \eta_k \tag{20}$$

Given a SINR threshold γ_{th}, the coverage probability of the network can be expressed as

$$C_{\mathrm{cov}}(\gamma_{th}) = \Pr\left(\mathrm{SINR}_k \geq \gamma_{th}\right) \tag{21}$$

In Monte Carlo simulation,

$$\hat{C}_{\mathrm{cov}} = \frac{1}{K}\sum_{k=1}^{K} 1\left(\mathrm{SINR}_k \geq \gamma_{th}\right) \tag{22}$$

where

$$1\cdot\left(\mathrm{SINR}_k \geq \gamma_{th}\right) = \begin{cases} 1, & \text{condition is satisfied} \\ 0, & \text{otherwise} \end{cases} \tag{23}$$

Using the UE's SE equation in (19), the UE throughput τ is given as

$$\tau_k = B\eta_k \tag{24}$$

where B is the available bandwidth. Thus, the aggregate network throughput becomes

$$\tau_{\mathrm{sum}} = \sum_{k=1}^{K} \tau_k \tag{25}$$

Finally, for a system-level comparison, the total network latency S can be modeled as the aggregate of the UE's transmission, propagation, processing and queueing components such that

$$S_k = S_{\mathrm{tx,k}} + S_{\mathrm{prop}} + S_{\mathrm{proc}} + S_{\mathrm{queue,k}} \tag{26}$$

The transmission latency $S_{\mathrm{tx,k}} = \frac{J_{\mathrm{pkt}}}{\eta_k}$, where J_{pkt} denotes the packet size in bits and the queueing component $S_{\mathrm{queue,k}} = \frac{Q_{\mathrm{k}}}{\eta_k}$, where Q_{k} represents the number of queued bits.

Thus, the total latency can be expressed as

$$S_{\mathrm{k}} = \frac{J_{\mathrm{pkt}} + Q_{\mathrm{k}}}{\eta_k} + S_{\mathrm{prop}} + S_{\mathrm{proc}} \tag{27}$$

3. RESULTS AND DISCUSSION

This section discusses the comparison between the three simulation scenarios having (a) one cell with a single 64-antenna AP placed in a cellular arrangement, (b) 64 single-antenna APs in one cell, and (c) cell-free mMIMO scenario comprising same AP locations as in (b).

The simulation setup has a total coverage area of 1000 m $\times$ 1000 m, to emulate ultra-dense network. A single UE is randomly dropped uniformly in the area while the SNRs in the uplink are computed as expressed in (6), (10), (14) and (18). In our assumption, the transmit power and noise power are, respectively $p = 23$ dBm and $\sigma_{\mathrm{ul}}^2 = -86.98$ dBm. The power levels are reasonably chosen for bandwidth value of 10 MHz. Furthermore, during computation of the propagation distance, we also assume deployment of the APs to be 10 m far above the UEs.

The cumulative distribution function (CDF) of the SNR obtained randomly at different locations by the UE is depicted in Figure 2. It can be observed that in the case of single-cell mMIMO, SNR variations of 50dB are realized. Hence, highest variation values occur when the UE is directly below the AP, while UE at the corner produces the lowest values. However, the cell-free network has comparatively much smaller SNR variations, basically due to shorter distances to the closest AP than in the case of mMIMO.

Taking a closer look at the figure shows higher SNR values practically everywhere around UE locations. A deeper look at the figure also depicts precisely the cell-free network to guarantee $\geq$ 24.5 dB of SNR at 95% of all UE locations as against 6.5 dB guaranteed for mMIMO. The mMIMO becomes the better option at the upper parts of the CDF curve which invariably are the locations of the most advantaged UEs. This shows the benefit of the mMIMO over cell-free network, which is clearly noticeable in the proximity of UEs to the 64-antenna in the former, as against a UE being close only to a few AP antennas per time in the latter.

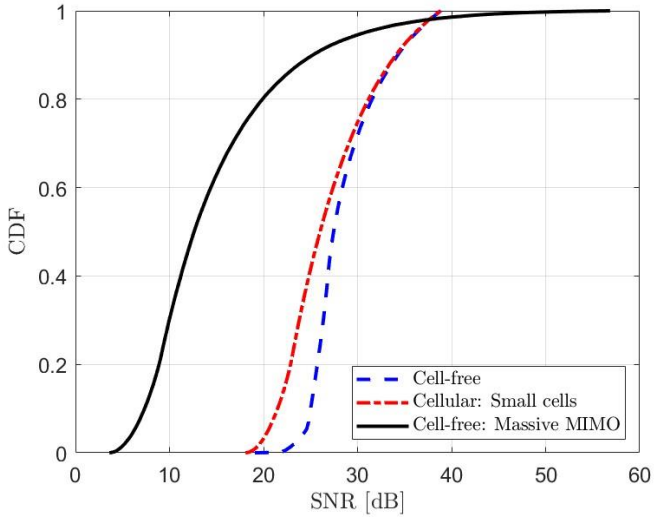


Figure 2: Plot of SNR achieved by a UE in each of the simulated three scenarios, giving rise to the CDFs based on random selection of UE location uniformly in the area.

It also follows from the expressions, analytically that higher SNR is achieved by the cell-free network as against the corresponding small-cell case. The difference can be seen in the upper end of the curve as having negligible value. This part corresponds to the point where the UE maintains closeness to a single AP out of many, creating one dominant term in (14), while producing a gap of 4 dB in the 95% probable SNR. The conclusion drawn from here is the preference of distributed antennas to large co-located arrays. Therefore, to be convinced that cell-free approach possesses great practical benefit, there is need to further perform analysis, using multiple UEs in order to introduce interference between concurrent transmissions.

In Figure 3, the effect of APs number on the performances of small cells, single cell mMIMO and cell-free networks are investigated, in terms of the average net throughput.

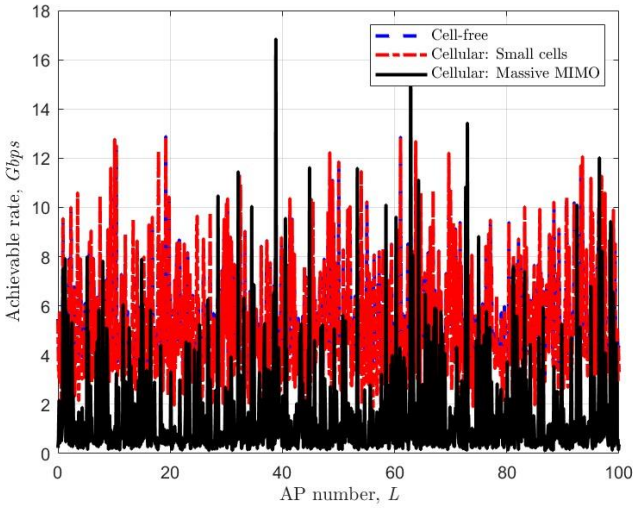


Figure 3: Achievable rate versus the number of APs for the three scenarios, showing the variation in aggregate network rate with increasing AP deployment.

This average is consistently acquired over the large-scale fading model as described in (5). As expected, cell-free networks clearly outperform both the small cell and single cell mMIMO systems. One of the reasons for this better performance is due to favourable propagation experienced by the cell-free, which results in less interference suffered compared to small cells. Hence, for all APs, it can be concluded that cell-free networks provide a significantly better performance than small cells and single cell mMIMO.

Also, the effect of user-level data rate distribution, radio link reliability and delay performance is investigated. Figure 4(a) illustrates the superiority of cell-free mMIMO over cell free and traditional cellular schemes across the simulated SNR range. The performance enhancement experienced by cell-free mMIMO can be attributed to the combination of multi antenna array gain and distributed AP cooperation. Conversely, in the small cell architecture, the association of a UE with one BS often results in poor SINR due to blockade and severe path loss, especially for UE located near cell boundaries. Consequently, the spatial degree of freedom provided by cell-free mMIMO architecture through beamforming and array gains improves interference management. This further increases the probability that a UE has access to at least one favourable AP by allowing several distributed APs to jointly serve UEs.

Based on strong dependence of the small cell on the serving BS, which degrades their SINR as depicted earlier, Figure 4(b) illustrates the benefit of equipping cell-free mMIMO with multiple antennas over single antenna scenarios experienced both in small cells and cell free architecture. As can be seen, the cell-free mMIMO curve exhibits a quick leftward displacement, indicating higher throughput achieved by larger proportion of UEs. This advantage demonstrates a significant importance for B5G and 6G applications requiring ubiquitous connectivity, while maintaining high capacity.

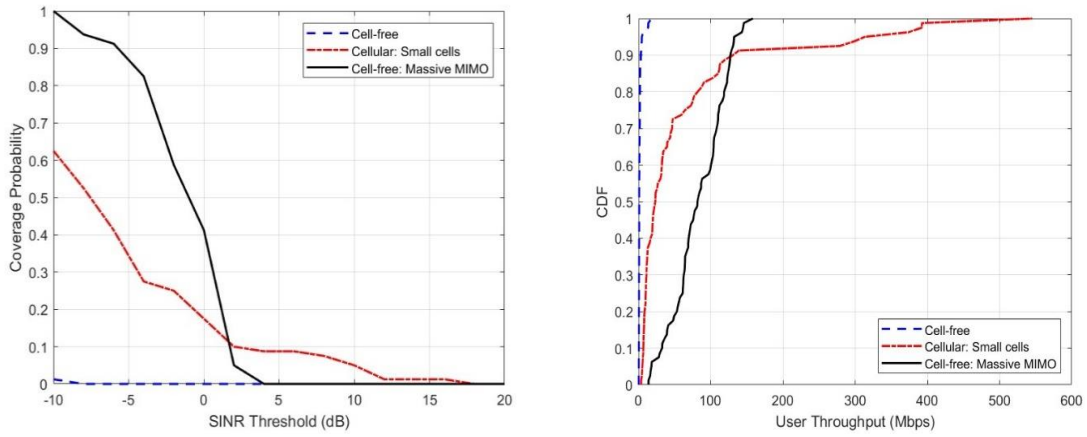


Figure 4: (a) Plot of coverage probability and SINR threshold for the three architectures, illustrating the variation in the proportion of users achieving the required SINR as the threshold increases, with cell-free mMIMO maintaining the highest coverage probability across the evaluated SINR range and (b) The CDF of per user throughput, showing the distribution of user-level throughput and the corresponding performance variation across the three considered 6G networks.

Figure 5(a) shows the average SE per UE as a function of the total number of UEs. It can be seen that cell-free mMIMO consistently provides the highest SE. The superior performance of cell-free mMIMO originates from concurrent addition of multiple antennas at each distributed AP, thereby exploiting spatial beamforming and array gain to improve the effective channel. Hence, as the UE population increases, cell-free architecture experiences more SE degradation, while establishing an unpredictable trend in small cells. Consequently, the slower SE degradation observed for cell-free mMIMO indicates greater scalability with user density which further demonstrates suitability for dense 6G deployment.
Finally, Figure 5(b) shows the CDF of user latency across the three architectures under consideration. It follows that the traditional small cell architecture possesses the highest latency due to poor SINR experienced by UEs requiring more time to transmit the same amount of information. However, this problem is alleviated by the cell-free network through distributed transmission. Overall, cell-free mMIMO provides additional reduction through spatial multiplexing and beamforming gains. These characteristics place cell-free mMIMO ahead of other schemes as an attractive candidate for latency sensitive B5G and 6G tasks such as machine-type communications, industrial automation, immersive communications and highly tactile applications.

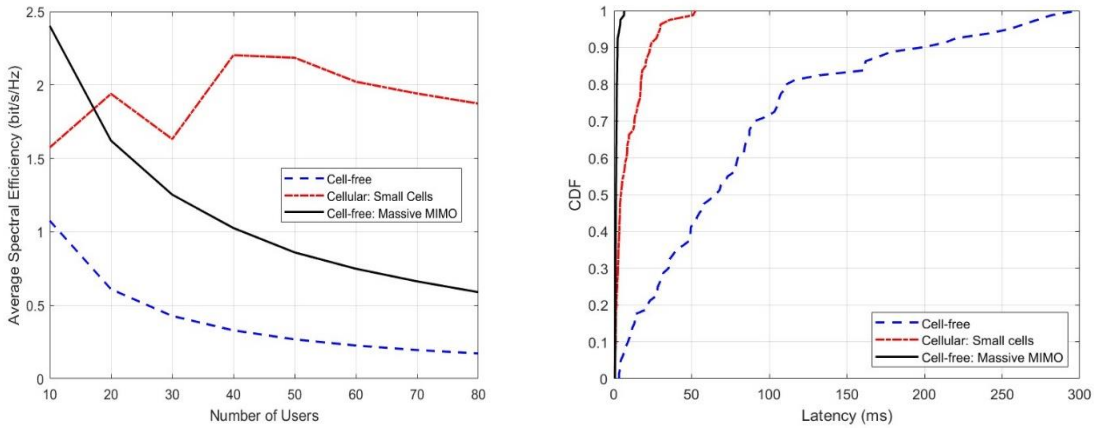


Figure 5: (a) SE of the network versus the number of UE, depicting the variation in network SE with increasing user density and the comparative performance of the three considered 6G architectures and (b) The CDF of UE latency describing the distribution of latency experienced by the UE and the comparative performance across the three considered 6G scenarios.

Table 1 summarizes the key quantitative findings obtained from the three simulation scenarios. The results show that cell-free mMIMO achieves consistently improved performance across the key 6G network indicators, including SE, user throughput, coverage probability and latency. Notably, the result shows 32.24% improvement in average SE, increasing from 0.639 bit/s/Hz for traditional cellular small cells to 0.845 bit/s/Hz for cell-free mMIMO. Similarly, average user throughput increases from 63.949 Mbps to 84.489 Mbps, representing 32.12% gain. In addition, the performance increment in the 5%-likely throughput moved from 5.516 Mbps to 18.382 Mbps, corresponding to 233.25% improvement. Also, average latency decreases from 9.867 ms to 1.707 ms, representing 82.70% reduction, while the coverage probability increases from 17.50% to 41.25%, corresponding to 135.71% relative improvement.

Table 1: Key quantitative findings from the simulation of the three network scenarios.

KPIs	**Cellular small cells**	**Cell-free**	**Cell-free mMIMO**	**Cell-free mMIMO vs small cells**
Average SINR	−6.101 dB	−20.976 dB	−1.547 dB	+4.554 dB
Spectral efficiency	0.639 bit/s/Hz	0.018 bit/s/Hz	0.845 bit/s/Hz	+32.24%
Average throughput	63.949 Mbps	1.840 Mbps	84.489 Mbps	+32.12%
5%-likely throughput	5.516 Mbps	0.314 Mbps	18.382 Mbps	+233.25%
Average latency	9.867 ms	83.159 ms	1.707 ms	82.70% reduction
95%-latency	29.815 ms	259.233 ms	3.828 ms	87.16% reduction
Coverage probability	17.50%	0.00%	41.25%	+135.71%

4. CONCLUSION

In this work, we analysed the performance evaluation of cell-free and traditional cellular small cell systems and their benefits under correlated shadow fading using Monte-Carlo simulations. We also compared the three scenarios of small cells, cell free and cell-free mMIMO networks in terms of achievable rate, SE, coverage probability and latency. Through analytical results, cell-free mMIMO improved average SE by 32.24% and throughput by 32.12% over traditional cellular network, while reducing average latency by 82.70% and increasing coverage probability by 23.7% points. However, cellular small cell systems require much less backhaul compared to cell-free mMIMO, thereby having more advantage in terms of implementation complexity. Future work will consider integrating artificial intelligence (AI) with the cell-free mMIMO architecture to increase scalability and reduce the implementation complexity. The AI-assisted resource allocation framework will be developed to dynamically optimize AP-UE cooperation, transmit power, beamforming and spectrum allocation according to instantaneous traffic and channel conditions. Furthermore, a more realistic 3GPP compatible 6G channel models such as larger user populations, mobility and blockage scenarios, imperfect channel state information and fronthaul limitations will be incorporated. The aim is to establish whether the observed analytical results remain consistent under more realistic 6G deployment conditions.

REFERENCES

[1] D. X. Chu, D. D. Lopez-Perez, P. Y. Yang, and D. F. Gunnarsson, *Heterogeneous Cellular Networks: Theory, Simulation and Deployment*. USA: Cambridge University Press, 2013.

[2] W. Jiang and H. D. Schottent, "A Heterogeneous Massive MIMO Technique for Uniform Service in Cellular Networks," in *ICC 2026 - IEEE International Conference on Communications*, May 2026, pp. 1–6. doi: 10.1109/ICC59461.2026.11587777.

[3] A. Ghosh *et al*., "Heterogeneous cellular networks: From theory to practice," *Commun. Mag. IEEE*, vol. 50, no. 6, pp. 54–64, 2012.

[4] C.-X. Wang *et al*., "Cellular architecture and key technologies for 5G wireless communication networks," *Commun. Mag. IEEE*, vol. 52, no. 2, pp. 122–130, 2014.

[5] T. E. Bogale and L. B. Le, "Massive MIMO and mmWave for 5G Wireless HetNet: Potential Benefits and Challenges," *IEEE Veh. Technol. Mag.*, vol. 11, no. 1, pp. 64–75, Mar. 2016, doi: 10.1109/MVT.2015.2496240.

[6] A. He, L. Wang, Y. Chen, M. Elkashlan, and K. K. Wong, "Massive MIMO in K-Tier Heterogeneous Cellular Networks: Coverage and Rate," in *2015 IEEE Global Communications Conference (GLOBECOM)*, Dec. 2015, pp. 1–6. doi: 10.1109/GLOCOM.2015.7417732.

[7] H. Farhadi, C. Wang, and M. Skoglund, "Distributed Transceiver Design and Power Control for Wireless MIMO Interference Networks," *IEEE Trans. Wirel. Commun.*, vol. 14, no. 3, pp. 1199–1212, Mar. 2015, doi: 10.1109/TWC.2014.2365202.

[8] V. Jungnickel *et al.*, "The role of small cells, coordinated multipoint, and massive MIMO in 5G," *Commun. Mag. IEEE*, vol. 52, no. 5, pp. 44–51, 2014.

[9] H. Q. Ngo, A. Ashikhmin, H. Yang, E. G. Larsson, and T. L. Marzetta, "Cell-Free Massive MIMO: Uniformly great service for everyone," in *2015 IEEE 16th International Workshop on Signal Processing Advances in Wireless Communications (SPAWC)*, Stockholm, Sweden: IEEE, Jun. 2015, pp. 201–205. doi: 10.1109/SPAWC.2015.7227028.

[10] M. Bashar, H. Q. Ngo, A. G. Burr, D. Maryopi, K. Cumanan, and E. G. Larsson, "On the Performance of Backhaul Constrained Cell-Free Massive MIMO with Linear Receivers," in *2018 52nd Asilomar Conference on Signals, Systems, and Computers*, Pacific Grove, CA, USA: IEEE, Oct. 2018, pp. 624–628. doi: 10.1109/ACSSC.2018.8645433.

[11] M. Ajmal, A. Siddiqa, M. A. Tariq, M. M. Saad, and D. Kim, "Dynamic Backhaul Clustering for Enhanced Scalability in Cell-Free Massive MIMO Networks," in *Proceedings of the 39th ACM/SIGAPP Symposium on Applied Computing*, Avila Spain: ACM, Apr. 2024, pp. 1735–1741. doi: 10.1145/3605098.3635914.

[12] F. Ndimumahoro and K. Ishibashi, "Cooperative Detection for Cell-Free Massive MIMO With Multiple Central Processing Units Under Backhaul Capacity Limitation," *IEEE Access*, vol. 13, pp. 90034–90051, 2025, doi: 10.1109/ACCESS.2025.3571649.

[13] A. Burr, M. Bashar, and D. Maryopi, "Cooperative Access Networks: Optimum Fronthaul Quantization in Distributed Massive MIMO and Cloud RAN - Invited Paper," in *2018 IEEE 87th Vehicular Technology Conference (VTC Spring)*, Porto: IEEE, Jun. 2018, pp. 1–5. doi: 10.1109/VTCSpring.2018.8417560.

[14] A. De La Oliva, J. A. Hernandez, D. Larrabeiti, and A. Azcorra, "An overview of the CPRI specification and its application to C-RAN-based LTE scenarios," *IEEE Commun. Mag.*, vol. 54, no. 2, pp. 152–159, Feb. 2016, doi: 10.1109/MCOM.2016.7402275.

[15] Y. Chu *et al.*, "Testbed Development: An Intelligent O-RAN-Based Cell-Free MIMO Network," *IEEE Commun. Mag.*, vol. 63, no. 6, pp. 74–81, Jun. 2025, doi: 10.1109/MCOM.001.2400574.

[16] S. Buzzi, F. Linsalata, E. Moro, and G. Interdonato, "Why User-Centric Cell-Free Distributed MIMO Systems Will be the Disruptive 6G Technology," *IEEE Commun. Mag.*, pp. 1–7, 2026, doi: 10.1109/MCOM.001.2500355.

[17] A. S. Mohammed, K. S. Tharakan, H. A. Ammar, H. ElSawy, and H. S. Hassanein, "Fronthaul Network Planning for Hierarchical and Radio-Stripes-Enabled CF-mMIMO in O-RAN," *IEEE Trans. Wirel. Commun.*, vol. 25, pp. 14781–14796, 2026, doi: 10.1109/TWC.2026.3678907.

[18] Ö. T. Demir, M. Masoudi, E. Björnson, and C. Cavdar, "Cell-Free Massive MIMO in O-RAN: Energy-Aware Joint Orchestration of Cloud, Fronthaul, and Radio Resources," *IEEE J. Sel. Areas Commun.*, vol. 42, no. 2, pp. 356–372, Feb. 2024, doi: 10.1109/JSAC.2023.3336187.

[19] Ö. T. Demir, E. Björnson, and L. Sanguinetti, "Foundations of User-Centric Cell-Free Massive MIMO," *Found. Trends® Signal Process.*, vol. 14, no. 3–4, pp. 162–472, 2021, doi: 10.1561/2000000109.